
Towards Bounding Causal Effects under Markov Equivalence

Alexis Bellot

Google DeepMind, London, UK

Abstract

Predicting the effect of unseen interventions is a fundamental research question across the data sciences. It is well established that, in general, such questions cannot be answered definitively from observational data, *e.g.*, as a consequence of unobserved confounding. A generalization of this task is to determine non-trivial bounds on causal effects induced by the data, also known as the task of *partial causal identification*. In the literature, several algorithms have been developed for solving this problem. Most, however, require a known parametric form or a fully specified causal diagram as input, which is usually not available in practical applications. In this paper, we assume as input a less informative structure known as a Partial Ancestral Graph, which represents a Markov equivalence class of causal diagrams and is learnable from observational data. In this more “data-driven” setting, we provide a systematic algorithm to derive bounds on causal effects that can be computed analytically.

1 Introduction

Causal relations are a prominent paradigm to describe our interactions with the world around us and underpin many concepts throughout all aspects of human enquiry, many of which are increasingly relevant for designing safe artificial intelligence (AI) systems. At the center of the notion of causality lies the idea of manipulation or intervention, *e.g.*, “what would happen to outcome Y if X were set to x ?”. For example, a physician might be interested in how a biomarker Y responds to a new dosage x of drug X . Alterna-

tively, an economist might wonder about the trajectory of economic indicators Y under an interest rate hike $X = x$ in a given country $Z = z$. Despite the disparate nature of these questions they all appeal to the same formal machinery, namely, they aim at establishing facts about (conditional) *causal effects*, *e.g.*, written $P_x(y | z)$.

In general, it is impossible to infer the effect of interventions from data alone (without physically manipulating reality) as further domain knowledge or assumptions are typically needed to uniquely pin down causal effects. This motivates the study of a problem known as (*partial*) *causal identification* (Pearl, 2009). The idea is to combine data from an observational distribution $P(\mathbf{V})$ with partial knowledge of the domain, articulated as a causal diagram, to bound a causal effect $P_x(y | z)$ within a tight, non-trivial interval. In other words, the problem is to infer a set of values that contains all effects implied by the causal models consistent with the data and assumptions. If the effect can be uniquely determined it is said to be point identified and the interval reduces to a single value. Several methods and algorithms to partially identify causal effects exist in the literature. The earliest bounds were developed under a set of instrumental variable assumptions (Robins, 1989; Manski, 1990). This approach has since been generalized to bound causal effects in sequential decision-making settings and for more general causal diagrams (Zhang and Bareinboim, 2019; Zhang, 2020). In parallel, several authors have shown that with a sufficiently expressive parameterization of the underlying causal model, bounds can also be computed by making inference of latent variables with bounded cardinality, with recent proposals developing polynomial optimization programs (Balke and Pearl, 1997; Hu et al., 2021; Padh et al., 2022; Li and Pearl, 2022) and Bayesian methods (Chickering and Pearl, 1996; Zhang et al., 2021; Finkelstein and Shpitser, 2020). All existing partial identification methods, however, rely on knowledge of a *fully* specified causal diagram. In practice, this formulation is often found too rigid as generally knowledge of a fully specified causal diagram is unrealistic. A sensible concern therefore is that forcing a single

diagram may lead to false modeling assumptions and, consequently, misleading inferences on causal effects.

In the spirit of designing more “data-driven” AI systems, one approach to circumvent the need for prior knowledge is to learn the causal diagram from data first, and then perform identification from there. The statistical constraints found in data (e.g. conditional independencies) can be leveraged to infer a class of *Markov equivalent* (ME) causal diagrams that is commonly represented as a *Partial Ancestral Graph* (PAG) (Richardson and Spirtes, 2002; Spirtes et al., 2000; Zhang, 2008b). For example, the PAG \mathcal{P} in Fig. 1b encodes the ME class of causal diagrams that is consistent with \mathcal{G} in Fig. 1a. In \mathcal{P} the directed edges encode ancestral relations, not necessarily direct, and the circle marks stand for structural uncertainty. Directed edges labeled with v signify the absence of unmeasured confounders. Identification from PAGs is of increasing interest. Several recent techniques for the *point* identification of causal effects have been developed (Zhang, 2008a,b; Jaber et al., 2018a; Hyttinen et al., 2015; Perkovic et al., 2018; Jaber et al., 2019b, 2018b) including a calculus and complete algorithms (Jaber et al., 2019a, 2022).

In this paper, we pursue a generalization of the partial identification task that consists of bounding causal effects with more restricted domain knowledge in the form of a class of ME causal diagrams (instead of a fully specified causal diagram). This notion is “data driven” in the sense that equivalence classes can, in principle, be inferred from observational data $P(\mathbf{V})$ only, and therefore corresponding bounds are based solely on constraints that can be inferred from finite samples, without additional domain knowledge. Our contributions can be summarized as follows. (1) We provide the first analytical expressions (closed-form, in terms of $P(\mathbf{V})$) for lower and upper bounds on a causal effect of interest given observational data based on the structure of a PAG. (2) We investigate enumeration strategies, *i.e.* the strategy of listing ME causal diagrams and performing partial identification on each diagram separately using existing “diagram-specific” bounding techniques. We show that, in fact, a large portion of ME causal diagrams could be shown to be “redundant” for the purpose of bounding causal effects. Despite this simplification, still, in the worst-case, an exponential number of graphs must be considered in general, which suggests that enumeration strategies are computationally intractable.

2 Background

The framework that underpins causal effects and diagrams rests on *structural causal models* (SCMs)

(Pearl, 2009, Def. 7.1.1). A SCM \mathcal{M} is a tuple $\langle \mathbf{V}, \mathbf{U}, \mathcal{F}, P(\mathbf{U}) \rangle$, where \mathbf{V} is a set of endogenous (observed) variables, \mathbf{U} is a set of exogenous latent variables, and $\mathcal{F} = \{f_V\}_{V \in \mathbf{V}}$ is a set of functions such that f_V determines values of V taking as argument variables $\mathbf{Pa}_V \subseteq \mathbf{V}$ and $\mathbf{U}_V \subseteq \mathbf{U}$, *i.e.* $V \leftarrow f_V(\mathbf{Pa}_V, \mathbf{U}_V)$. Values of \mathbf{U} are drawn from an exogenous distribution $P(\mathbf{u})$. We assume the model to be recursive, *i.e.* that there are no cyclic dependencies among the variables. Following standard practice, functional dependencies are represented by a causal diagram \mathcal{G} over \mathbf{V} in which we omit exogenous nodes and add a bi-directed dashed arc between two endogenous nodes if they share an exogenous parent, see *e.g.* Fig. 1a. An intervention on a subset $\mathbf{X} \subset \mathbf{V}$, denoted by $do(\mathbf{x})$, is an operation that fixes values of \mathbf{X} to constants \mathbf{x} , replacing the functions $\{f_X : X \in \mathbf{X}\}$ that would normally determine their values. Let $\mathcal{M}_{\mathbf{x}}$ denote the model induced by action $do(\mathbf{x})$. Accordingly, $\mathcal{M}_{\mathbf{x}}$ induces a corresponding interventional distribution over \mathbf{V} , denoted $P_{\mathbf{x}}(\mathbf{V})$. Similarly, $P_{\mathbf{x}}(\mathbf{Y} \mid \mathbf{Z})$ denotes the conditional distribution of \mathbf{Y} given \mathbf{Z} in model $\mathcal{M}_{\mathbf{x}}$. Domains of \mathbf{V} are discrete and finite.

Equivalence classes. One common graphical abstraction to represent sets of causal diagrams with the same d -separation¹ and non-ancestral relations are so called maximal ancestral graphs (MAGs). “Ancestral” due to the fact that MAGs does not contain directed cycles, *i.e.*, directed paths that start and end at the same node, or almost directed cycles, *i.e.*, directed paths $X \rightarrow \dots \rightarrow Y$ such that $X \leftarrow \dots \rightarrow Y$ and “maximal” due to the fact that every pair of nonadjacent nodes (X, Y) , there exists a set $\mathbf{Z} \subset \mathbf{V}$ that d -separates them.

Two causal diagrams or MAGs are said to be *Markov equivalent* (ME) if they entail the same set of d -separations. A ME class of graphs can be summarized in a PAG that includes one additional edge tip “ \circ ” that denotes undecidability, *i.e.*, there are graphs in the equivalence class with both types of edge tips (Zhang, 2006, 2008a)². Directed edges $X \rightarrow Y$ in a MAG or PAG are said to be visible, denoted $X \overset{v}{\rightarrow} Y$, if unobserved confounding can be ruled out. For example, the PAG in Fig. 1b encodes the ME class of the causal diagram in Fig. 1a. The output of the FCI algorithm is a PAG that can be recovered consistently under an assumption of *faithfulness* (Spirtes et al., 2000; Zhang, 2006, 2008a).

Graphical notions in PAGs. It will be useful to use standard graph-theoretic family abbreviations to represent graphical relationships in causal diagrams or

¹The criterion of d -separation follows (Pearl, 2009, Def. 1.2.3).

²Selection bias, typically represented with undirected edges (Zhang, 2008b), is not considered in this paper.

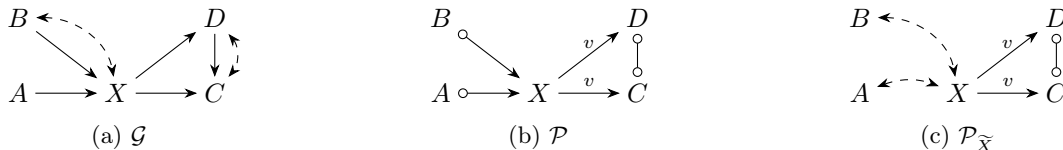


Figure 1: Examples of diagrams.

equivalence classes. A path between X and Y is *potentially directed* (causal) from X to Y if there is no arrowhead on the path pointing towards X . Y is called a *possible descendant* of X , *i.e.*, $Y \in \text{PossDe}(X)$, and X a *possible ancestor* of Y , *i.e.*, $X \in \text{PossAn}(Y)$, if there is a potentially directed path from X to Y . By stipulation, $X \in \text{PossAn}(X)$. A set \mathbf{X} is ancestral if no node outside \mathbf{X} is a possible ancestor of any node in \mathbf{X} . X is called a possible parent of Y , *i.e.*, $X \in \text{PossPa}(Y)$, and Y a possible child of X , *i.e.*, $Y \in \text{PossCh}(X)$, if they are adjacent and the edge is not into X . Further, X is called a possible spouse of Y , *i.e.*, $X \in \text{PossSp}(Y)$, if they are adjacent and the edge is not visible. For a set of nodes \mathbf{X} , we have $\text{PossPa}(\mathbf{X}) = \bigcup_{X \in \mathbf{X}} \text{PossPa}(X)$. If the edge marks on a path between X and Y are all circles, we call the path a circle path. We refer to the closure of nodes connected with circle paths as a bucket. For example, in Fig. 1b $\{C, D\}$ is a bucket.

Let \mathcal{P} denote a PAG over \mathbf{V} and $\mathbf{X} \subseteq \mathbf{V}$. $\mathcal{P}_{\mathbf{X}}$ denotes the induced subgraph of \mathcal{P} over \mathbf{X} . The \mathbf{X} -lower-manipulation of \mathcal{P} deletes all those edges that are visible in \mathcal{P} and are out of variables in \mathbf{X} , replaces all those edges that are out of variables in \mathbf{X} but are invisible in \mathcal{P} with bi-directed edges, and otherwise keeps \mathcal{P} as it is. The resulting graph is denoted as $\mathcal{P}_{\underline{\mathbf{X}}}$. The \mathbf{X} -upper-manipulation of \mathcal{P} deletes all those edges in \mathcal{P} that are into variables in \mathbf{X} , and otherwise keeps \mathcal{P} as it is. The resulting graph is denoted as $\mathcal{P}_{\overline{\mathbf{X}}}$. The \mathbf{X} -tilde-upper-manipulation of \mathcal{P} deletes all those edges that are visible in \mathcal{P} and are into variables in \mathbf{X} , replaces all those edges that are into variables in \mathbf{X} but are invisible in \mathcal{P} with bi-directed edges, and otherwise keeps \mathcal{P} as it is. The resulting graph is denoted as $\mathcal{P}_{\tilde{\mathbf{X}}}$. An example is given in Fig. 1c.

3 Identification of causal effects

In this section, we review the techniques developed in (Jaber et al., 2019a) for *point-identifying* (conditional) causal effects. We start by defining a decomposition of variables \mathbf{V} into so called c -components that forms the basis for systematic identification algorithms (Tian and Pearl, 2002, Lemma 11). In a causal diagram, two nodes are said to be in the same c -component $\mathbf{C} \subseteq \mathbf{V}$ if and only if they are connected by a bi-directed path, *i.e.* composed entirely

of edges of the type “ $\leftarrow\text{---}\rightarrow$ ”. For any set $\mathbf{C} \subseteq \mathbf{V}$, $Q[\mathbf{C}] := P_{\mathbf{v} \setminus \mathbf{c}}(\mathbf{c})$ denotes the post-interventional distribution of \mathbf{C} under an intervention on $\mathbf{V} \setminus \mathbf{C}$. By definition $Q[\mathbf{V}] = P(\mathbf{v})$ and by convention $Q[\emptyset] = 1$.

The notion of pc -component, defined below, generalizes that of c -components to equivalence classes and will be important for the proposed approach. In words, the pc -component of a set \mathbf{A} includes all the nodes which could, in some causal diagram, be in the c -component of some node in \mathbf{A} .

Definition 1 (pc -component). *In a PAG, or any induced subgraph thereof, two nodes are in the same possible c -component (pc -component) if there is a path between them such that all non-endpoint nodes along the path are colliders, and none of the edges is visible.*

Following this definition, *e.g.*, A, B and X in Fig. 1b are in the same pc -component since X is a collider on the path between them and none of the edges are visible. By contrast, A and C are not in the same pc -component since there is a visible edge on all paths that connect them. In particular, it holds that X and Y are in the same c -component in a Markov equivalent causal diagram \mathcal{G} , then X and Y are in the same pc -component in its PAG. Using these notions, a target quantity $Q[\mathbf{C}]$ can be decomposed into a product of smaller quantities, as shown in Prop. 1 using the Region construct (Def. 2) from Jaber et al. (2019a).

Definition 2 (Region). *Given a PAG \mathcal{P} over \mathbf{V} , and $\mathbf{A} \subseteq \mathbf{C} \subseteq \mathbf{V}$. Let the region of \mathbf{A} with respect to \mathbf{C} , denoted $\mathcal{R}_{\mathbf{A}}^{\mathbf{C}}$, be the union of the buckets that contain nodes in the pc -component of \mathbf{A} in the sub-graph $\mathcal{P}_{\mathbf{C}}$.*

Proposition 1 (Thm. 1 (Jaber et al., 2019a)). *Given a PAG \mathcal{P} over \mathbf{V} and $\mathbf{A} \subseteq \mathbf{C} \subseteq \mathbf{V}$. $Q[\mathbf{C}]$ can be decomposed as,*

$$Q[\mathbf{C}] = \frac{Q[\mathcal{R}_{\mathbf{A}}^{\mathbf{C}}] \cdot Q[\mathcal{R}_{\mathbf{C} \setminus \mathbf{A}}^{\mathbf{C}}]}{Q[\mathcal{R}_{\mathbf{A}}^{\mathbf{C}} \cap \mathcal{R}_{\mathbf{C} \setminus \mathbf{A}}^{\mathbf{C}}]}. \quad (1)$$

Identification of quantities $Q[\cdot]$ given an equivalence class \mathcal{P} uses a notion of (partial) topological order over the nodes in \mathcal{P} . A partial topological order is defined on buckets rather than individual nodes therefore extending the notion used in single causal diagrams and is valid for all causal diagrams in the Markov equivalence class (Jaber et al., 2018a, Lemma 1). For exam-

ple, $A < B < X < \{C, D\}$, is a partial topological order over the buckets of \mathcal{P} in Fig. 1b.

Conditional causal effects, of the form $P_{\mathbf{x}}(\mathbf{y} | \mathbf{z})$, can be similarly be decomposed using the notion of $Q[\cdot]$ by the definition of conditional probability,

$$P_{\mathbf{x}}(\mathbf{y} | \mathbf{z}) = \sum_{\mathbf{c} \setminus \mathbf{y}} \left(Q[\mathbf{C} \cup \mathbf{Z}] / \sum_{\mathbf{c}} Q[\mathbf{C} \cup \mathbf{Z}] \right), \quad (2)$$

where $\mathbf{C} = \text{PossAn}(\mathbf{Y} \cup \mathbf{Z})_{\mathcal{P}_{\mathbf{V} \setminus \mathbf{X}}} \setminus \mathbf{X}$. Complete identification algorithms for both unconditional and conditional causal effects from a PAG exist based on the decomposition in Prop. 1 (Jaber et al., 2019a, 2022).

4 Partial identification of causal effects

We introduce the task of partial identification of a causal effect from an observational distribution and knowledge of a PAG that represents a set of compatible causal diagrams. This notion generalizes the model-specific definition of partial identification.

Definition 3. *The causal effect from \mathbf{X} to \mathbf{Y} given \mathbf{Z} is said to be partially identifiable from a PAG \mathcal{P} if $P(\mathbf{v})$ determines a bound $P_{\mathbf{x}}(\mathbf{y} | \mathbf{z}) \in [a, b]$ that is strictly contained in $[0, 1]$ and is valid given any causal diagram in the Markov equivalence class represented by \mathcal{P} .*

Let $\mathbb{M}(\mathcal{P})$ denote the set of SCMs \mathcal{M} with causal diagrams in \mathcal{P} . In general, therefore, different SCMs $\mathcal{M} \in \mathbb{M}(\mathcal{P})$ with generated distribution $P(\mathbf{V})$, i.e. $P(\mathbf{V}) = P(\mathbf{V}; \mathcal{M})$, imply different post-interventional distributions $P_{\mathbf{x}}(\mathbf{y} | \mathbf{z}; \mathcal{M})$ or $Q[\mathbf{C}; \mathcal{M}] := P_{\mathbf{v} \setminus \mathbf{c}}(\mathbf{c}; \mathcal{M})$. In other words, one cannot uniquely determine post-interventional distributions from observational data (regardless of how many samples are collected). As surveyed in the previous section, decompositions based on $Q[\cdot]$ and induced subgraphs of the PAG play a critical role in identification. For the task of partial identification, these will similarly play an important role. As a result of the completeness of systematic identification algorithms based on the decomposition in Prop. 1, a query $P_{\mathbf{x}}(\mathbf{y} | \mathbf{z})$ is identifiable if and only if all of the corresponding $Q[\cdot]$ in the query’s decomposition are identifiable. On the contrary, one or more $Q[\cdot]$ will witness the non-identifiability.

Our next results introduce bounds on components $Q[\mathbf{S}]$, $\mathbf{S} \subset \mathbf{C}$ in terms of larger (identifiable) components $Q[\mathbf{C}]$ that can be plugged into the decomposition of causal effects of Prop. 1.

Proposition 2 (Lower bound). *Given a PAG \mathcal{P} , consider sets $\mathbf{S} \subset \mathbf{C} \subseteq \mathbf{V}$ and define $\mathbf{W} = \text{PossAn}(\mathbf{S})_{\mathcal{P}_{\mathbf{C}}}$,*

Algorithm 1 Partial IDP

Input: A PAG \mathcal{P} and disjoint sets $\mathbf{X}, \mathbf{Y} \subset \mathbf{V}$

Output: Lower and upper-bound expressions for $P_{\mathbf{x}}(\mathbf{y})$

- 1: Let $\mathbf{D} := \text{PossAn}(\mathbf{Y})_{\mathcal{P}_{\mathbf{V} \setminus \mathbf{X}}}$
 - 2: **return** $\sum_{\mathbf{d} \setminus \mathbf{y}} \text{PartialID}(\mathbf{D}, \mathbf{V}, P)$
 - 3: **function** $\text{PartialID}(\mathbf{C}, \mathbf{T}, Q = Q[\mathbf{T}])$
 - 4: if $\mathbf{C} = \emptyset$ then return 1.
 - 5: if $\mathbf{C} = \mathbf{T}$ then return Q .
 - /* In $\mathcal{P}_{\mathbf{T}}$, let \mathbf{B} denote a bucket, and let $\mathbf{C}_{\mathbf{B}}$ denote the pc -component of \mathbf{B} */
 - 6: **if** $\exists \mathbf{B} \subset \mathbf{T} \setminus \mathbf{C}$ such that $\mathbf{C}_{\mathbf{B}} \cap \text{PossCh}(\mathbf{B})_{\mathcal{P}_{\mathbf{T}}} \subseteq \mathbf{B}$ **then**
 - 7: Compute $Q[\mathbf{T} \setminus \mathbf{B}]$ from $Q[\mathbf{T}]$ via (Jaber et al., 2018a, Prop. 2).
 - 8: **return** $\text{PartialID}(\mathbf{C}, \mathbf{T} \setminus \mathbf{B}, Q[\mathbf{T} \setminus \mathbf{B}])$
 - 9: **else if** $\exists \mathbf{B} \subset \mathbf{C}$ such that $\mathcal{R}_{\mathbf{B}} \neq \mathbf{C}$ **then**
 - 10: **return** $\frac{\text{PartialID}(\mathcal{R}_{\mathbf{B}}, \mathbf{T}, Q) \times \text{PartialID}(\mathcal{R}_{\mathbf{C} \setminus \mathcal{R}_{\mathbf{B}}}, \mathbf{T}, Q)}{\text{PartialID}(\mathcal{R}_{\mathbf{B}} \cap \mathcal{R}_{\mathbf{C} \setminus \mathcal{R}_{\mathbf{B}}}, \mathbf{T}, Q)}$
 - 11: **else**
 - 12: **return** Lower and upper bounds for $Q[\mathbf{C}]$ from $Q[\mathbf{T}]$ via Props. 2 and 3.
 - 13: **end if**
-

$\mathbf{R} = \mathbf{W} \setminus \mathbf{S}$, and $\mathbf{T} = \text{PossSp}(\mathbf{S})_{\mathcal{P}_{\mathbf{C}}} \setminus \mathbf{S}$. Let \mathbf{A}, \mathbf{B} partition \mathbf{R} such that $\mathbf{B} = \text{PossDe}(\mathbf{T})_{\mathcal{P}_{\mathbf{C}}} \cap \mathbf{R}$, $\mathbf{A} = \mathbf{R} \setminus \mathbf{B}$. $Q[\mathbf{S}]$ is lower bounded as follows:

$$Q[\mathbf{S}] \geq \max_{\mathbf{z}} \frac{Q[\mathbf{W}]}{\sum_{\mathbf{s}, \mathbf{b}} Q[\mathbf{W}]}, \quad (3)$$

where $\mathbf{Z} = \text{PossPa}(\mathbf{W})_{\mathcal{P}} \setminus \text{PossPa}(\mathbf{S})_{\mathcal{P}}$.

Proposition 3 (Upper bound). *Given a PAG \mathcal{P} , consider sets $\mathbf{S} \subset \mathbf{C} \subseteq \mathbf{V}$ and let a partial topological ordering of \mathbf{S} be $\mathbf{S}_1 < \dots < \mathbf{S}_k$. Define $\mathbf{W} = \text{PossAn}(\mathbf{S})_{\mathcal{P}_{\mathbf{C}}}$, $\mathbf{R} = \mathbf{W} \setminus \mathbf{S}$, and $\mathbf{T} = \text{PossSp}(\mathbf{S})_{\mathcal{P}_{\mathbf{C}}} \setminus \mathbf{S}$. Let \mathbf{A}, \mathbf{B} partition \mathbf{R} such that $\mathbf{B} = \text{PossDe}(\mathbf{T})_{\mathcal{P}_{\mathbf{C}}} \cap \mathbf{R}$, $\mathbf{A} = \mathbf{R} \setminus \mathbf{B}$. $Q[\mathbf{S}]$ is upper bounded as follows:*

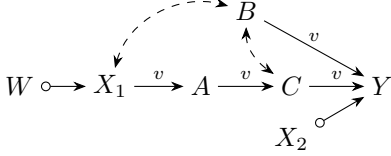
$$Q[\mathbf{S}] \leq \min_{\mathbf{z}} \left\{ \frac{Q[\mathbf{W}]}{\sum_{\mathbf{s}, \mathbf{b}} Q[\mathbf{W}]} - \sum_{\mathbf{s}_k} \frac{Q[\mathbf{W}]}{\sum_{\mathbf{s}, \mathbf{b}} Q[\mathbf{W}]} \right\} + Q[\mathbf{S} \setminus \mathbf{S}_k], \quad (4)$$

where $\mathbf{Z} = \text{PossPa}(\mathbf{W})_{\mathcal{P}} \setminus \text{PossPa}(\mathbf{S})_{\mathcal{P}}$.

Among the quantities in the above equations, we could establish that $Q[\mathbf{W}] = \sum_{\mathbf{c} \setminus \mathbf{w}} Q[\mathbf{C}]$ is identifiable from $Q[\mathbf{C}]$ by the following proposition.

Proposition 4. *Let $\mathbf{W} \subseteq \mathbf{C} \subset \mathbf{V}$ such that $\mathbf{W} = \text{PossAn}(\mathbf{W})_{\mathcal{P}_{\mathbf{C}}}$. Then, $Q[\mathbf{W}] = \sum_{\mathbf{c} \setminus \mathbf{w}} Q[\mathbf{C}]$.*

Alg. 1 provides a systematic procedure to bound causal effects by extending the complete identification algorithm IDP (Jaber et al., 2019a) with a call to the


 Figure 2: \mathcal{P}

propositions above (line 12) whenever a component is not uniquely identifiable.

Proposition 5. *Partial IDP (Alg. 1) terminates and is sound.*

The proof follows from the soundness of IDP (Jaber et al., 2019a) and Props. 2 and 3. A similar algorithm for partially identifying conditional causal effects could be derived by adapting CIDP (conditional IDP) (Jaber et al., 2022) with a call to the propositions above whenever a component is not uniquely identifiable.

4.1 Example 1

Consider the query $P_{x_1, x_2}(y)$ given \mathcal{P} in Fig. 2. We will proceed by decomposing the query into smaller components and either uniquely identify or bound each term as appropriate. Using the c -factor notion $Q[\cdot]$, we have that $P_{x_1, x_2}(y) = \sum_{a, b, c, w} P_{x_1, x_2}(y, a, b, c, w) = \sum_{a, b, c, w} Q[Y, A, B, C, W]$; which can be simplified as $Q[Y, A, B, C] = \sum_w Q[Y, A, B, C, W]$ since the set $\{Y, A, B, C\}$ is ancestral in the sub-graph $\mathcal{P}_{\{Y, A, B, C, W\}}$ by Prop. 4. Then, considering the pc -component structure of induced sub-graphs following Prop. 1, we have, in a first instance, that $Q[Y, A, B, C] = Q[A]Q[Y, B, C]$ as the region of A in $\mathcal{P}_{\{A, Y, B, C\}}$ is $\mathcal{R}_A^{\{A, Y, B, C\}} = \{A\}$, the region of $\{Y, B, C\}$ in the same sub-graph is $\mathcal{R}_{\{Y, B, C\}}^{\{A, Y, B, C\}} = \{Y, B, C\}$, and have an empty intersection. With a similar call to Prop. 1, we have $Q[Y, B, C] = Q[Y]Q[B, C]$ where $Q[B, C] = \sum_{x_1, w} Q[W, X_1, B, C]$. $Q[W, X_1, B, C]$ is identifiable from \mathcal{P} in line 7 of Alg. 1 which returns $P(c \mid a, x_1, b, w)P(x_1, b, w)$.

One remaining component: $Q[Y]$, is left to be computed, which, however, is not identifiable from $P(\mathbf{v})$ as calls to lines 6 and 9 in Alg. 1 fail, due to the potential presence of an unobserved confounder between X_2 and Y . Props. 2 and 3 gives us a strategy to bound $Q[Y]$ from a larger identifiable component, namely $Q[Y, X_2] = P(x_2)P(y \mid x_2, c, b)$. In particular, using the notation in the propositions we have that $\mathbf{W} = \text{PossAn}(Y)_{\mathcal{P}_{Y, X_2}} = \{Y, X_2\}$, $\mathbf{R} = \mathbf{W} \setminus \mathbf{S} = \{Y, X_2\} \setminus \{Y\} = \{X_2\}$. \mathbf{R} could be partitioned into $\mathbf{A} = \emptyset$ and $\mathbf{B} = \{X_2\}$ as X_2 is confounded with Y due to the edge $X_2 \circ \rightarrow Y$. As a consequence, $\sum_{s, b} Q[\mathbf{W}] = 1$. Moreover, $\text{PossPa}(\mathbf{W}) \setminus \text{PossPa}(Y) = \emptyset$. Putting

these findings into Eqs. (3) and (4), we get that $Q[Y] \geq Q[Y, X_2]$ and $Q[Y] \leq Q[Y, X_2] + 1 - Q[X_2]$, where $Q[X_2] = \sum_y Q[Y, X_2] = P(x_2)$.

Finally, putting each term in the expression $P_{x_1, x_2}(y) = \sum_{a, b, c} Q[A]Q[Y]Q[B, C]$ together we have the lower bound,

$$P_{x_1, x_2}(y) \geq \sum_{a, b, c} P(y \mid x_2, b, c)P(x_2)P(a \mid x_1) \times \sum_{w, x_1} P(w, b, x_1)P(c \mid a, w, b, x_1), \quad (5)$$

and the upper bound,

$$P_{x_1, x_2}(y) \leq \sum_{a, b, c} (P(y \mid x_2, b, c)P(x_2) + 1 - P(x_2)) \times P(a \mid x_1) \sum_{w, x_1} P(w, b, x_1)P(c \mid a, w, b, x_1). \quad (6)$$

4.2 Example 2

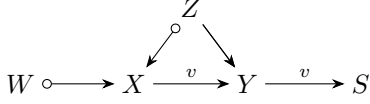
Consider the query $P_{x, w, z}(y)$ given \mathcal{P} in Fig. 3. We have that $P_{x, w, z}(y) = \sum_s P_{x, w, z, s}(y) = \sum_s Q[Y, S] = Q[Y]$ as Y is ancestral in the subgraph $\mathcal{P}_{\{Y, S\}}$. $Q[Y]$, however, is not identifiable in \mathcal{P} , as the path $Z \rightarrow Y$ start with an invisible edge (that doesn't rule out unobserved confounding) (Jaber et al., 2019a, Thm. 3). The pc -component that contains Y is given by $\{W, X, Z, Y\}$. It follows that $Q[W, X, Z, Y]$ is identifiable given the PAG as a call to line 7 in Alg. 1, evaluating $Q[W, X, Z, Y]$ from $Q[W, X, Z, Y, S] = P(w, x, z, y, s)$ using (Jaber et al., 2018a, Prop. 2), returns $P(w, x, y, z)$. Following Props. 2 and 3, $Q[Y]$ could be bounded as a function of $Q[W, X, Z, Y]$. We have in particular that $\mathbf{W} = \text{PossAn}(Y)_{\mathcal{P}_{W, X, Z, Y}} = \{W, X, Z, Y\}$ and $\mathbf{R} = \{W, X, Z, Y\} \setminus \{Y\} = \{W, X, Z\}$ which can be partitioned into $\mathbf{A} = \{W\}$, $\mathbf{B} = \{X, Z\}$ since $\{W\}$ is not a possible descendant of any possible spouse of Y in \mathcal{P} . $\text{PossPa}(\mathbf{W}) \setminus \text{PossPa}(Y) = \{W\}$. As a consequence, we have that

$$Q[Y] \geq \max_w \frac{Q[W, X, Z, Y]}{\sum_{z, x, y} Q[W, X, Z, Y]}. \quad (7)$$

Equivalently $P_{x, w, z}(y) \geq \max_w P(z, y, x \mid w)$. Moreover,

$$Q[Y] \leq 1 + \min_w \left\{ \frac{Q[W, X, Z, Y]}{\sum_{z, y, x} Q[W, X, Z, Y]} - \sum_y \frac{Q[W, X, Z, Y]}{\sum_{z, y, x} Q[W, X, Z, Y]} \right\}, \quad (8)$$

or equivalently $P_{x, w, z}(y) \leq \min_w \{P(z, y, x \mid w) - P(z, x \mid w)\} + 1$.


 Figure 3: \mathcal{P}

4.3 Applications in biology and health

We exemplify in this section the inference that could be made on real-world examples.

We revisit the protein signalling study of (Sachs et al., 2005). Signalling pathways regulate the activity of a cell. The ability to precisely predict the effect of perturbations in signalling pathways, *e.g.*, by knocking out a gene that inactivates a protein in the network, on a phenotype of interest, such as cell growth, can have important applications for the treatment of disease. We consider computing bounds on the effect of PKC inactivation on the RAF/MEK/ERK pathway given the PAG in Fig. 4b recovered from phosphorylation data (*i.e.* markers of pathway activation)³. The query of interest is given by $P(\text{RAF}, \text{MEK}, \text{ERK} \mid \text{do}(\text{PKC}))$. Using the $Q[\cdot]$ notion, we then have that $P(\text{RAF}, \text{MEK}, \text{ERK} \mid \text{do}(\text{PKC})) = \sum_{\text{PKA}} Q[\text{RAF}, \text{MEK}, \text{ERK}, \text{PKA}] = \sum_{\text{PKA}} Q[\text{RAF}, \text{ERK}, \text{PKA}]Q[\text{MEK}]$. Notice that AKT can be marginalized out as $\{\text{RAF}, \text{MEK}, \text{ERK}, \text{PKA}\}$ is ancestral in the corresponding PAG. In this expression $Q[\text{MEK}] = P(\text{MEK} \mid \text{RAF})$ is identifiable but $Q[\text{RAF}, \text{ERK}, \text{PKA}]$ isn't; although it could be bounded from a larger identifiable component such as $Q[\text{RAF}, \text{ERK}, \text{PKA}, \text{PKC}]$. The identification formula for this component is given in line (7) of Alg. 1, specifically: $Q[\text{RAF}, \text{ERK}, \text{PKA}, \text{PKC}] = P(\text{RAF}, \text{ERK}, \text{PKA}, \text{PKC}, \text{MEK})/P(\text{MEK} \mid \text{RAF})$. Following the notation of Props. 2 and 3, in $\mathcal{P}_{\{\text{RAF}, \text{ERK}, \text{PKA}, \text{PKC}\}}$, $\mathbf{W} = \text{PossAn}(\mathbf{S}) = \{\text{RAF}, \text{ERK}, \text{PKA}, \text{PKC}\}$, $\mathbf{R} = \mathbf{B} = \{\text{PKC}\}$, and $\mathbf{Z} = \emptyset$. It then follows that,

$$Q[\text{RAF}, \text{ERK}, \text{PKA}] \geq Q[\text{RAF}, \text{ERK}, \text{PKA}, \text{PKC}]. \quad (9)$$

Further,

$$Q[\text{RAF}, \text{ERK}, \text{PKA}] \leq Q[\text{RAF}, \text{ERK}, \text{PKA}, \text{PKC}] - \sum_{\text{ERK}} Q[\text{RAF}, \text{ERK}, \text{PKA}, \text{PKC}] + Q[\text{RAF}, \text{PKA}]. \quad (10)$$

$Q[\text{RAF}, \text{PKA}]$ could be further upper-bounded from $Q[\text{RAF}, \text{PKA}, \text{PKC}]$ with a similar strategy; in particular giving $Q[\text{RAF}, \text{PKA}] \leq Q[\text{RAF}, \text{PKA}, \text{PKC}] + 1 - Q[\text{PKC}] = P(\text{RAF}, \text{PKA}, \text{PKC}) + 1 - P(\text{PKC})$.

With these expressions, for instance, we could infer probabilities of high and low pathway activation after

³We use a discretized version of the data following (Hartemink et al., 2000) with levels: high (2), average (1), low (0) activation.

knocking out, *i.e.* intervening on, PKC:

$$P(\text{RAF} = 0, \text{MEK} = 0, \text{ERK} = 0 \mid \text{do}(\text{PKC} = 0)) \in [0.0214, 0.0864], \quad (11)$$

$$P(\text{RAF} = 2, \text{MEK} = 2, \text{ERK} = 2 \mid \text{do}(\text{PKC} = 0)) \in [0.1120, 0.3115], \quad (12)$$

respectively. In turn, by relying on the current consensus biological network (Sachs et al., 2005, Fig. 2), given in Fig. 4a, the causal effects would be point estimated to be 0.0441 and 0.1861 respectively. Without committing to a particular causal diagram, the inferred bounds would be the more cautious conclusion on causal effects.

Next, we consider an adaptation of the Lung Cancer diagram from (Lauritzen and Spiegelhalter, 1988), shown in Fig. 4c. We are interested in determining the effect of a chemotherapy treatment (C) for lung cancer (L) on dyspnoea (D), *i.e.* breathing difficulty, in the context of other factors such as smoking (unobserved and represented with a bi-directed edge), pollution (P), age (A), and Tuberculosis (T). For this experiment, we generate 1,000 samples from a compatible SCM. With knowledge of the causal diagram in Fig. 4c and 1,000 observational data points independently sampled from $P(C, L, D, P, A)$, the causal effect can be approximated to be $P(d = 1 \mid \text{do}(c = 1)) = P(d = 1 \mid c = 1) = 0.7775$. However, with knowledge of the PAG inferred from data, given in Fig. 4d, we could only partially identify the causal effect with the proposed bounds. In this case, $P(d \mid \text{do}(c)) = \sum_{l,a,p,t} Q[D, L, A, P, T]$ which, following Props. 2 and 3, is lower-bounded by $\sum_{l,a,p,t} Q[D, L, A, P, T, C] = P(d, c)$ and upper-bounded by $\sum_{l,a,p,t} Q[D, L, A, P, T, C] + 1 - \sum_{l,a,p,t} Q[C, L, A, P, T] = P(d, c) + 1 - P(c)$.

These expressions imply that knowledge of the PAG and observational data license the following approximate bounds,

$$P(d = 1 \mid \text{do}(c = 1)) \in [0.5087, 0.9353]. \quad (13)$$

In this example, therefore, the observational data alone already suggests that chemotherapy treatment is more likely to cause breathing difficulty on average than not cause breathing difficulty.

5 The difficulty of enumerating causal diagrams from a PAG

The techniques explored so far overlook the potential for listing (relevant) ME causal diagrams and subsequently applying existing (partial) identification techniques given each diagram separately. Listing all ME

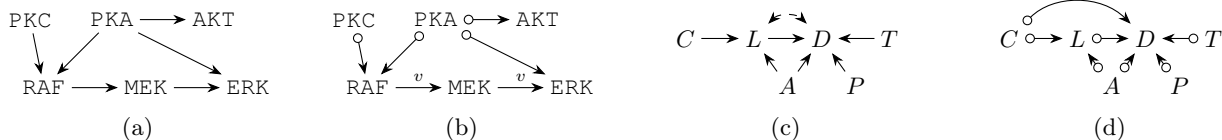


Figure 4: (a) Protein signalling network (Sachs et al., 2005, Fig. 2), (b) PAG; (c) Lung Cancer causal diagram, (d) PAG.



Figure 5: Diagrams used in Sec. 5.

causal diagrams is exponentially costly, and intractable in general even with an assumption of no unobserved confounding, *i.e.* in the space of directed acyclic graphs (Wienöbst et al., 2023). However, a number of observations can be made to avoid listing all ME causal diagrams which reduce the space of diagrams to a (potentially tractable) *subset* of “relevant” ME causal diagrams without loss of generality.

This section explores the definition of sets of ME causal diagrams $\mathcal{K} \subset \mathcal{P}$ with the distinctiveness of being equally expressive in the sense that,

$$\left\{ P_{\mathbf{x}}(\mathbf{y} \mid \mathbf{z}; \mathcal{M}) : \mathcal{M} \in \mathbb{M}(\mathcal{P}) \right\} = \left\{ P_{\mathbf{x}}(\mathbf{y} \mid \mathbf{z}; \mathcal{M}) : \mathcal{M} \in \mathbb{M}(\mathcal{K}) \right\}, \quad (14)$$

for a given causal effect $P_{\mathbf{x}}(\mathbf{y} \mid \mathbf{z})$. Under Eq. (14), minimum and maximum values of causal effects remain unchanged, and one may exploit \mathcal{K} instead of \mathcal{P} for inference. The hope is that if the set of causal diagrams \mathcal{K} is small enough then we might be able to apply existing partial identification algorithms on every causal diagram $\mathcal{G} \in \mathcal{K}$ efficiently.

We start by introducing the notion of a Loyal Equivalent Graph (LEG) (Def. 4), from (Zhang and Spirtes, 2012, Prop. 2), that are sets of ME MAGs that retain “expressiveness” in the sense of Eq. (14). This result is given in Prop. 6.

Definition 4. *Given a MAG \mathcal{G} , there exists a ME MAG \mathcal{H} , called a Loyal Equivalent Graph, such that all bi-directed edges in \mathcal{H} are invariant, and every directed edge in \mathcal{G} is also in \mathcal{H} .*

Proposition 6 (Expressiveness of LEGs). *Given a PAG \mathcal{P} , let \mathcal{L} be the set of ME LEGs. Then, $\mathbb{M}(\mathcal{P}) = \mathbb{M}(\mathcal{L})$.*

For example, the LEG in Fig. 5c is derived from the MAG in Fig. 5b by replacing the bi-directed edge with a directed one. Prop. 6 shows that the set of ME LEGs is as expressive as the set of ME MAGs that are en-

coded by \mathcal{P}^4 . The significance of this proposition lies in the fact that ME LEGs are a subset of ME MAGs and that, contrary to ME MAGs, ME LEGs are in principle listable by exhaustively applying a simple criterion for the reversal of directed edges while remaining Markov equivalent, *i.e.* (Zhang and Spirtes, 2012, Lemma 2). We review this criterion in more detail in Appendix A and give an algorithm for listing ME LEGs that exploits it in Appendix D.

A second redundancy result is given in Prop. 7 by introducing so called *maximally bi-directed* (MBD) diagrams.

Definition 5. *A causal diagram \mathcal{G} is said to be maximally bi-directed if no further bi-directed edges can be added without breaking a d -separation.*

Proposition 7 (Expressiveness of MBD diagrams). *Given a PAG \mathcal{P} , let \mathcal{D} be the set of ME MBD diagrams. Then, $\mathbb{M}(\mathcal{P}) = \mathbb{M}(\mathcal{D})$.*

MBD causal diagrams can be constructed from an LEG by adding bi-directed edges on top of invisible directed edges wherever possible. For example, the causal diagram \mathcal{G} in Fig. 5d, compatible with the LEG L in Fig. 5c, is said to be maximally bi-directed as no further bi-directed edges can be added while remaining Markov equivalent. \mathcal{G} has the distinctiveness of inducing a family of SCMs which includes all SCMs that are compatible with any causal diagram compatible with the corresponding LEG L in Fig. 5c, *i.e.* $\mathbb{M}(\mathcal{G}) = \mathbb{M}(L)$. More specifically, in this example, \mathcal{G} induces a class of SCMs given by: $x := f_X(\mathbf{u}_{X,Y})$, $z := f_Z(\mathbf{u}_{X,Z})$, $y := f_Y(x, z, \mathbf{u}_{X,Z}, \mathbf{u}_{X,Y})$, with deterministic functions and exogeneous distributions arbitrarily defined. We can see that this parameterization is flexible enough to represent any SCM induced by causal diagrams compatible with L . As a consequence, in general, Prop. 7 implies that the set of ME MBD causal diagrams is as expressive as the set of *all* ME causal diagrams.

⁴Recall, as noted in Sec. 2, that MAGs (and LEGs) encode the sets of causal diagrams that would be represented by the same MAG (or LEG).

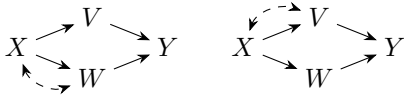


Figure 6: Diagrams used in Prop. 8.

Appendix D gives an algorithm for generating all ME MBD diagrams \mathcal{D} from the set of all ME LEGs \mathcal{L} .

Additionally, note that in general multiple MBD causal diagrams can be derived from with a single LEG. For example, Fig. 6 gives two MBD causal diagrams induced by the same LEG (both bi-directed edges could not appear simultaneously as that would violate the independence $V \perp\!\!\!\perp W \mid X$). Therefore, unfortunately, a reduction of the set of ME MBD diagrams \mathcal{D} while preserving the space of SCMs $\mathbb{M}(\mathcal{D})$ is, in general, not possible. Multiple MBD diagrams for each LEG may have to be considered to properly characterize causal effects given a PAG \mathcal{P} .

Proposition 8 (Non-redundancy). *Given a PAG \mathcal{P} , let \mathcal{G} and \mathcal{H} be two MBD diagrams constructed from a ME LEG. In general, $\mathbb{M}(\mathcal{G}) \not\subseteq \mathbb{M}(\mathcal{H})$ and $\mathbb{M}(\mathcal{H}) \not\subseteq \mathbb{M}(\mathcal{G})$.*

In other words, bounds for a given causal effect computed given two MBD diagrams will in general be different and one has to consider both diagrams to correctly characterize bounds on causal effects given an equivalence class. The proof proceeds by exploiting the MBD causal diagrams in Fig. 6 as a counter-example. As a consequence of this result, we conjecture that enumeration techniques, in the worst-case, would have to consider all MBD diagrams separately. The algorithms we propose for listing LEGs and MBD causal diagrams suggests that doing so requires a polynomial cost in the number of edges for LEGs, in addition to the computational cost of bounding algorithms themselves that can involve a number of parameters that is exponential in the number of variables. This analysis suggests that existing bounding techniques, even with the consideration of redundancies presented in this section, are not practical beyond a handful of variables.

6 Conclusions and discussion

Causal effect estimation is a common inference problem across many different applications, many of which do not have a known causal diagram describing the system of variables. In this paper, we study the problem of partial identification with knowledge of a Markov equivalence class, represented by a Partial Ancestral Graph (PAG), that can be inferred from data. We demonstrate that analytical bounds can be derived by exploiting the invariances present in the PAG and the corresponding decomposition of causal effects. These

are the first bounds on causal effects in the literature applicable without knowledge of a fully-specified causal diagram. We further consider enumeration techniques, that list relevant causal diagrams and apply partial identification techniques on each one separately, by showing that although several redundancies exist within the space of ME causal diagrams, the computational cost remains exponential in practice. Ultimately, with these results we hope to widen the practice of causal effect inference without the necessity of making strong assumptions about the domain of interest. In such scenarios, the expectation (or rather hope) is that causal effects could be *partially* identifiable, that is that non-trivial bounds on causal effects can be inferred.

References

- Balazadeh Meresht, V., Syrgkanis, V., and Krishnan, R. G. (2022). Partial identification of treatment effects with implicit generative models. *Advances in Neural Information Processing Systems*, 35:22816–22829.
- Balke, A. and Pearl, J. (1997). Bounds on treatment effects from studies with imperfect compliance. *Journal of the American Statistical Association*, 92(439):1171–1176.
- Bellot, A. and van der Schaar, M. (2021). Deconfounded score method: Scoring dags with dense unobserved confounding. *arXiv preprint arXiv:2103.15106*.
- Bellot, A., Zhang, J., and Bareinboim, E. (2022). Scores for learning discrete causal graphs with unobserved confounders. *Technical Report R-83, Causal AI Lab, Columbia University*.
- Chickering, D. M. and Pearl, J. (1996). A clinician’s tool for analyzing non-compliance. In *Proceedings of the National Conference on Artificial Intelligence*, pages 1269–1276.
- Finkelstein, N. and Shpitser, I. (2020). Deriving bounds and inequality constraints using logical relations among counterfactuals. In *Conference on Uncertainty in Artificial Intelligence*, pages 1348–1357. PMLR.
- Gunsilius, F. (2019). Bounds in continuous instrumental variable models. *arXiv preprint arXiv:1910.09502*, 1.
- Hartemink, A. J., Gifford, D. K., Jaakkola, T. S., and Young, R. A. (2000). Using graphical models and genomic expression data to statistically validate models of genetic regulatory networks. In *Biocomputing 2001*, pages 422–433. World Scientific.
- Hu, Y., Wu, Y., Zhang, L., and Wu, X. (2021). A generative adversarial framework for bounding confounded causal effects. In *Proceedings of the AAAI*

- Conference on Artificial Intelligence*, volume 35, pages 12104–12112.
- Hytinen, A., Eberhardt, F., and Järvisalo, M. (2015). Do-calculus when the true graph is unknown. In *UAI*, pages 395–404.
- Jaber, A., Ribeiro, A., Zhang, J., and Bareinboim, E. (2022). Causal identification under markov equivalence: calculus, algorithm, and completeness. *Advances in Neural Information Processing Systems*, 35:3679–3690.
- Jaber, A., Zhang, J., and Bareinboim, E. (2018a). Causal identification under markov equivalence. *arXiv preprint arXiv:1812.06209*.
- Jaber, A., Zhang, J., and Bareinboim, E. (2018b). A graphical criterion for effect identification in equivalence classes of causal diagrams. In *Proceedings of the Twenty-Seventh International Joint Conference on Artificial Intelligence*.
- Jaber, A., Zhang, J., and Bareinboim, E. (2019a). Causal identification under markov equivalence: Completeness results. In *International Conference on Machine Learning*, pages 2981–2989. PMLR.
- Jaber, A., Zhang, J., and Bareinboim, E. (2019b). Identification of conditional causal effects under markov equivalence. *Advances in Neural Information Processing Systems*, 32.
- Jung, Y., Tian, J., and Bareinboim, E. (2021). Estimating identifiable causal effects on markov equivalence class through double machine learning. In *International Conference on Machine Learning*, pages 5168–5179. PMLR.
- Lauritzen, S. L. and Spiegelhalter, D. J. (1988). Local computations with probabilities on graphical structures and their application to expert systems. *Journal of the Royal Statistical Society: Series B (Methodological)*, 50(2):157–194.
- Li, A. and Pearl, J. (2022). Bounds on causal effects and application to high dimensional data. In *Proceedings of the AAAI Conference on Artificial Intelligence*, volume 36, pages 5773–5780.
- Manski, C. F. (1990). Nonparametric bounds on treatment effects. *The American Economic Review*, 80(2):319–323.
- Padh, K., Zeitler, J., Watson, D., Kusner, M., Silva, R., and Kilbertus, N. (2022). Stochastic causal programming for bounding treatment effects. *arXiv preprint arXiv:2202.10806*.
- Pearl, J. (2009). *Causality*. Cambridge university press.
- Perkovic, E., Textor, J., Kalisch, M., and Maathuis, M. H. (2018). Complete graphical characterization and construction of adjustment sets in markov equivalence classes of ancestral graphs. *The Journal of Machine Learning Research*.
- Richardson, T. and Spirtes, P. (2002). Ancestral graph markov models. *The Annals of Statistics*, 30(4):962–1030.
- Robins, J. M. (1989). The analysis of randomized and non-randomized aids treatment trials using a new approach to causal inference in longitudinal studies. *Health service research methodology: a focus on AIDS*, pages 113–159.
- Sachs, K., Perez, O., Pe’er, D., Lauffenburger, D. A., and Nolan, G. P. (2005). Causal protein-signaling networks derived from multiparameter single-cell data. *Science*, 308(5721):523–529.
- Spirtes, P., Glymour, C. N., Scheines, R., and Heckerman, D. (2000). *Causation, prediction, and search*. MIT press.
- Tian, J. and Pearl, J. (2002). *A general identification condition for causal effects*. eScholarship, University of California.
- Tian, J. and Pearl, J. (2003). On the identification of causal effects. *Technical Report R-290L*.
- Wienöbst, M., Luttermann, M., Bannach, M., and Liskiewicz, M. (2023). Efficient enumeration of markov equivalent dags. In *Proceedings of the AAAI Conference on Artificial Intelligence*, volume 37, pages 12313–12320.
- Zhang, J. (2006). *Causal inference and reasoning in causally insufficient systems*. PhD thesis, Citeseer.
- Zhang, J. (2008a). Causal reasoning with ancestral graphs. *Journal of Machine Learning Research*, 9:1437–1474.
- Zhang, J. (2008b). On the completeness of orientation rules for causal discovery in the presence of latent confounders and selection bias. *Artificial Intelligence*, 172(16-17):1873–1896.
- Zhang, J. (2020). Designing optimal dynamic treatment regimes: A causal reinforcement learning approach. In *International Conference on Machine Learning*, pages 11012–11022. PMLR.
- Zhang, J. and Bareinboim, E. (2019). Near-optimal reinforcement learning in dynamic treatment regimes. *Advances in Neural Information Processing Systems*, 32.
- Zhang, J. and Spirtes, P. (2005). A characterization of markov equivalence classes for ancestral graphical models. *Carnegie Mellon University*.
- Zhang, J. and Spirtes, P. L. (2012). A transformational characterization of markov equivalence for directed acyclic graphs with latent variables. *arXiv preprint arXiv:1207.1419*.

Zhang, J., Tian, J., and Bareinboim, E. (2021).
Partial counterfactual identification from observational and experimental data. *arXiv preprint arXiv:2110.05690*.

A Background, related work, and limitations

A.1 Background

In this section, we review several graphical notions that are used or mentioned in the main body of this document.

Definition 6 (Maximal Ancestral Graph). *A mixed graph is ancestral if it does not contain directed or almost directed cycles. It is maximal if, for every pair of nonadjacent vertices (X, Y) , there exists a set $Z \subset V$ that d -separates them. A Maximal Ancestral Graph (MAG) is a graph that is both ancestral and maximal.*

Given a causal graph, a unique MAG over V can be constructed such that both independence and non-ancestral relations among V are retained; see e.g. (Zhang, 2008a, Sec. 3). Two MAGs are said to be Markov equivalent if they entail the same set of d -separations. Among Markov equivalent MAGs, a particular subset, called Loyal Equivalent Graphs (LEG), can be constructed with the fewest bi-directed edges, all of which are invariant, *i.e.* bi-directed edges in LEGs appear in all MAGs with the same d -separations and non-ancestral relations (Zhang and Spirtes, 2005, Corollary 18), and is given in Def. 4. Thus, between a MAG and its LEG, only one kind of difference is possible, namely, some bi-directed edges in the MAG are oriented as directed edges in its LEG, as illustrated in Fig. 7.



Figure 7: MAG (left), LEG (right)

We will use standard graph-theoretic family abbreviations to represent graphical relationships in causal diagrams \mathcal{G} , such as parents pa , descendants de , ancestors an , and spouses sp . For example, let $X \in sp(Y)_{\mathcal{G}}$ if $X \leftarrow\!\!\!\rightarrow Y$ is present in \mathcal{G} . Capitalized versions Pa, De, An, Sp include the argument as well, e.g. $Pa(\mathbf{X})_{\mathcal{G}} = pa(\mathbf{X})_{\mathcal{G}} \cup \mathbf{X}$. If $X \in an(Y)_{\mathcal{G}} \cap sp(Y)_{\mathcal{G}}$, we say that there is an almost directed cycle between X and Y . An important consequence of the definition of LEGs is that one can traverse the space of Markov equivalent LEGs by checking whether directed edges can be reversed with a simple criterion, restated below from (Zhang and Spirtes, 2012, Lemma 2).

Proposition 9 (Transformational characterization of LEGs). *Let \mathcal{G} be an arbitrary LEG, and $X \rightarrow Y$ an arbitrary directed edge in \mathcal{G} . The reversal of $X \rightarrow Y$ produces a Markov equivalent LEG if and only if $Pa(X)_{\mathcal{G}} = pa(Y)_{\mathcal{G}}$ and $Sp(X)_{\mathcal{G}} = Sp(Y)_{\mathcal{G}}$.*

Proof. The proof can be found in (Zhang and Spirtes, 2012). □

Two Markov equivalent LEGs can always be transformed to each other via a sequence of reversals according to Prop. 9. Similarly to the definition for PAGs, directed edges $X \rightarrow Y$ in a MAG are said to be visible if there exists no causal graph compatible with this MAG with an edge $X \leftarrow\!\!\!\rightarrow Y$, that is unobserved confounding between X and Y can be ruled out. Visibility of an edge can be easily determined by a graphical condition (Zhang, 2008a, Lemma 9). Directed edges that are not visible are called invisible. Prop. 9 is important because, although listing all Markov equivalent MAGs is in general infeasible, one could in principle list all Markov equivalent LEGs by checking reversal of invisible directed edges with this graphical criterion. An explicit algorithm for generating Markov equivalent LEGs is given in Appendix D.

Finally, we review manipulations in causal diagrams \mathcal{G} that will be used in the following proofs. Let \mathcal{G} denote a causal diagram over V and $\mathbf{X} \subseteq V$. $\mathcal{G}_{\mathbf{X}}$ denotes the induced subgraph of \mathcal{G} over \mathbf{X} . The \mathbf{X} -lower-manipulation of \mathcal{G} deletes all those edges that are out of variables in \mathbf{X} and otherwise keeps \mathcal{G} as it is. The resulting graph is denoted as $\underline{\mathcal{G}}_{\mathbf{X}}$. The \mathbf{X} -upper-manipulation of \mathcal{G} deletes all those edges in \mathcal{G} that are into variables in \mathbf{X} , and otherwise keeps \mathcal{G} as it is. The resulting graph is denoted as $\overline{\mathcal{G}}_{\mathbf{X}}$.

A.2 Related work

We review in this section related work concerned with bounding causal effects with knowledge of fully-specified graph, as no treatment of equivalence classes has been proposed yet.

The first informative bounds over the causal effects were derived (Robins, 1989; Manski, 1990) with a specific studies with imperfect compliance, under a set of instrumental variable assumptions. Derived bounds may be written in closed form and could be extended as a more general strategy for bounding causal effects in arbitrary graphs. This was demonstrated recently by (Zhang, 2020; Zhang and Bareinboim, 2019) in which the authors

extended earlier bounding strategies to estimate system dynamics in sequential decision-making settings and more general graphs.

In the literature, another line of research was pioneered by the seminal work of (Balke and Pearl, 1997) that employs a polynomial optimization program to compute causal bounds and are provably optimal. They proposed a family of canonical models with finite unobserved states, which sufficiently represent all observations and consequences of interventions in instrumental variable models. Based on this canonical characterization, (Balke and Pearl, 1997) reduced the bounding problem to a series of equivalent linear programs. (Chickering and Pearl, 1996) further used Bayesian techniques to investigate the sharpness of these bounds with regard to the observational sample size. Recently, (Zhang et al., 2021; Finkelstein and Shpitser, 2020) describe a polynomial programming approach to solve the partial identification for general causal graphs. They generalize the canonical characterization of SCMs to arbitrary graphs, although require discrete endogenous variables with small support as the time complexity of their algorithm grows exponentially with the size of the support set of variables. In continuous settings, (Gunsilius, 2019) extends the linear programming approach to partial identification of instrumental variable graphs with continuous treatments. Several recent works follow a similar approach: parameterizing causal effects as a linear combinations of a set of fixed basis functions (Padh et al., 2022) or neural networks (Balazadeh Meresht et al., 2022; Hu et al., 2021) and subsequently match the (moments of the) observed distribution while minimizing and maximizing causal effects.

A.3 Limitations

In this work, we start from the assumption that the true PAG that underlies a system of interest can be inferred from data. In general, this requires an assumption of faithfulness, *i.e.* that the independencies in data imply a corresponding separation in the underlying causal diagram, and an oracle for testing for conditional independencies. Learning the true PAG from finite data can be a significant challenge in practice (Spirtes et al., 2000; Bellot et al., 2022; Bellot and van der Schaar, 2021). In higher-dimensional systems, the computational complexity of estimating the conditional distributions that define lower and upper bounds on causal effects is another substantial challenge. In light of this, it is important to make the distinction between the task of partial identification, that is inferring an expression to bound causal effects, and that of causal effect estimation, that is providing efficient estimators from finite samples to compute bounds in practice. This set of results is concerned with the first task (partial identification). The objective of our procedure is to decide whether the effect can be bounded and provide an expression for lower and upper bounds, while being agnostic as to whether $P(\mathbf{V})$ can be accurately estimated from the available samples. Several works consider the efficient estimation of identifiable causal effects (Jung et al., 2021). Extending these techniques to the problem of bounding non-identifiable causal effects is an important direction for future work.

B Proofs

Prop. 1 restated. *Given a PAG \mathcal{P} over \mathbf{V} and $\mathbf{A} \subset \mathbf{C} \subseteq \mathbf{V}$. $Q[\mathbf{C}]$ can be decomposed as,*

$$Q[\mathbf{C}] = \frac{Q[\mathcal{R}_{\mathbf{A}}^{\mathbf{C}}] \cdot Q[\mathcal{R}_{\mathbf{C} \setminus \mathbf{A}}^{\mathbf{C}}]}{Q[\mathcal{R}_{\mathbf{A}}^{\mathbf{C}} \cap \mathcal{R}_{\mathbf{C} \setminus \mathbf{A}}^{\mathbf{C}}]}. \quad (15)$$

Proof. The proof can be found in (Jaber et al., 2019a, Thm.1). □

Lemma 1. *Given a PAG \mathcal{P} over \mathbf{V} , let $\mathbf{C} \subset \mathbf{V}$. Then,*

$$\left\{ Q[\mathbf{C}; \mathcal{M}] : \mathcal{M} \in \mathbb{M}(\mathcal{P}) \right\} = \left\{ Q[\mathbf{C}; \mathcal{M}] : \mathcal{M} \in \mathbb{M}(\mathcal{P}_{\overline{\mathbf{V} \setminus \mathbf{C}}}) \right\}. \quad (16)$$

Proof. For a given causal diagram \mathcal{G} , a causal effect of interest $P_{\mathbf{x}}(\mathbf{y})$ can be written,

$$P_{\mathbf{x}}(\mathbf{y}) = \sum_{\mathbf{v} \in \{\mathbf{x} \cup \mathbf{y}\}} \int_{\Omega_{\mathbf{U}}} \prod_{V \in \mathbf{V} \setminus \mathbf{X}} P(v \mid \mathbf{pa}_V, \mathbf{u}_V) dP(\mathbf{u}) = \sum_{\mathbf{s} \in \{\mathbf{y}\}} \int_{\Omega_{\mathbf{U}}} \prod_{V \in \mathbf{S}} P(v \mid \mathbf{pa}_V, \mathbf{u}_V) dP(\mathbf{u}),$$

where $\mathbf{S} = An(\mathbf{Y})_{\mathcal{G}_{\overline{\mathbf{X}}}} \setminus \mathbf{X}$ and \mathbf{s} is some value in the domain of \mathbf{S} . This expression depends only on probabilities associated with variables \mathbf{S} , $\mathbf{U}_{\mathbf{S}}$, $S \in \mathbf{S}$ and their functional dependencies through terms $P(v \mid \mathbf{pa}_V, \mathbf{u}_V)$ that

in turn are determined by the underlying SCMs compatible with the graph and data, which in this case are parameterized by $\{f_V : V \in \mathbf{S}\}$ and $\{P(u_V) : V \in \text{An}(\mathbf{S})_{\mathcal{G}[\mathbf{C}]}\}$ where \mathbf{C} is the c -component in \mathcal{G} that contains \mathbf{S} . The distribution and values of any other variable is of no consequence to the desired causal effect. In particular, any descendants of \mathbf{Y} in \mathcal{G} can be marginalized out without loss of generality.

The same reasoning applies to $Q[\mathbf{C}] := P_{\mathbf{v} \setminus \mathbf{c}}(\mathbf{c})$ which depends only on $\text{An}(\mathbf{C})_{\mathcal{G}_{\mathbf{V} \setminus \mathbf{C}}} \setminus (\mathbf{V} \setminus \mathbf{C})$ and the functional dependencies of associated variables. Recall that $\mathcal{P}_{\mathbf{V} \setminus \mathbf{C}}$ denotes the graph in which all edges that are visible in \mathcal{P} and are into variables in $\mathbf{V} \setminus \mathbf{C}$ are deleted, and in which all invisible edges that are into variables in $\mathbf{V} \setminus \mathbf{C}$ are replaced with bi-directed edges. Since $\mathcal{P}_{\mathbf{V} \setminus \mathbf{C}}$ only modifies the functional assignment of descendants of \mathbf{C} and these do not influence the causal effect of interest we have that,

$$\left\{ Q[\mathbf{C}; \mathcal{M}] : \mathcal{M} \in \mathbb{M}(\mathcal{P}) \right\} = \left\{ Q[\mathbf{C}; \mathcal{M}] : \mathcal{M} \in \mathbb{M}(\mathcal{P}_{\mathbf{V} \setminus \mathbf{C}}) \right\}. \quad (17)$$

□

This proposition implies that it is sufficient to consider the set of causal diagrams compatible with $\mathcal{P}_{\mathbf{V} \setminus \mathbf{C}}$, i.e. the set of ME causal diagrams \mathcal{G} in which edges $X \rightarrow Y, X \in \text{pa}(\mathbf{C})_{\mathcal{G}}, Y \in \mathbf{C}$ have been removed, to characterize lower and upper bounds over queries of the form $Q[\mathbf{C}]$ from \mathcal{P} . A useful corollary to this result is the following.

Prop. 2 restated. *Given a PAG \mathcal{P} , consider sets $\mathbf{S} \subset \mathbf{C} \subseteq \mathbf{V}$ and define $\mathbf{W} = \text{PossAn}(\mathbf{S})_{\mathcal{P}_{\mathbf{C}}}$, $\mathbf{R} = \mathbf{W} \setminus \mathbf{S}$, and $\mathbf{T} = \text{PossSp}(\mathbf{S})_{\mathcal{P}_{\mathbf{C}}} \setminus \mathbf{S}$. Let \mathbf{A}, \mathbf{B} partition \mathbf{R} such that $\mathbf{B} = \text{PossDe}(\mathbf{T})_{\mathcal{P}_{\mathbf{C}}} \cap \mathbf{R}, \mathbf{A} = \mathbf{R} \setminus \mathbf{B}$. $Q[\mathbf{S}]$ is lower bounded as follows:*

$$Q[\mathbf{S}] \geq \max_z \frac{Q[\mathbf{W}]}{\sum_{s,b} Q[\mathbf{W}]}, \quad (18)$$

where $\mathbf{Z} = \text{PossPa}(\mathbf{W})_{\mathcal{P}} \setminus \text{PossPa}(\mathbf{S})_{\mathcal{P}}$.

Proof. If $Q[\mathbf{S}]$ is not identifiable given \mathcal{P} , then $Q[\mathbf{S}]$ is not identifiable in one or more ME causal diagrams \mathcal{G} by (Jaber et al., 2019a, Thm. 4). In each of those diagrams \mathcal{G} , then there must exist an open backdoor path from a node in $\mathbf{V} \setminus \mathbf{S}$ to a node in \mathbf{S} that could be blocked with access to a set of unobserved confounders \mathbf{U} . Let \mathbf{U} be the union of exogenous variables that block such open backdoor paths. In turn, let $\mathbf{S} \subset \mathbf{C}$, where \mathbf{C} is a pc -component in a sub-graph of \mathcal{P} with $Q[\mathbf{C}]$ identifiable. Following the statement of the proposition, let $\mathbf{W} = \text{PossAn}(\mathbf{S})_{\mathcal{P}_{\mathbf{C}}}$, $\mathbf{R} = \mathbf{W} \setminus \mathbf{S}$, and $\mathbf{T} = \text{PossSp}(\mathbf{S})_{\mathcal{P}_{\mathbf{C}}} \setminus \mathbf{S}$. Further, let \mathbf{A}, \mathbf{B} partition \mathbf{R} such that $\mathbf{B} = \text{PossDe}(\mathbf{T})_{\mathcal{P}_{\mathbf{C}}}, \mathbf{A} = \mathbf{R} \setminus \mathbf{B}$. Without loss of generality, by Lem. 1 inference on $Q[\mathbf{S}]$ given \mathcal{P} is equivalent to inference on $Q[\mathbf{S}]$ given $\mathcal{P}_{\mathbf{V} \setminus \mathbf{S}}$.

To show the claim, we show that $Q[\mathbf{S}]$ is lower bounded in every causal diagram compatible with $\mathcal{P}_{\mathbf{V} \setminus \mathbf{S}}$. Let \mathcal{G} be any such causal diagram. In light of the definitions above, it holds that,

1. \mathbf{R} is d -separated from \mathbf{S} conditioned on \mathbf{U} in $\mathcal{G}_{\mathbf{V} \setminus \mathbf{W}, \mathbf{R}}$,
2. \mathbf{U} is exogenous and thus d -separated from \mathbf{R} conditioned on $\mathbf{V} \setminus \mathbf{W}$ in $\mathcal{G}_{\mathbf{V} \setminus \mathbf{W}, \mathbf{R}}$,
3. \mathbf{A} is d -separated from \mathbf{U} conditioned on $\mathbf{V} \setminus \mathbf{W}$ in $\mathcal{G}_{\mathbf{V} \setminus \mathbf{W}}$.

Condition (1) states that all backdoor paths from \mathbf{R} to \mathbf{S} , i.e. those starting with an edge $R \leftarrow \dots$ or $R \leftarrow \dots \rightarrow \dots, R \in \mathbf{R}$, are blocked conditioned on \mathbf{U} . To see this, note that \mathbf{U} is chosen to block all backdoor paths through an unobserved confounder and that any other backdoor paths are assumed away in $\mathcal{P}_{\mathbf{V} \setminus \mathbf{S}}$, i.e. there is no edge of the form $X \rightarrow Y, X \in \mathbf{S}, Y \in \mathbf{V} \setminus \mathbf{S}$ in any causal diagram compatible with $\mathcal{P}_{\mathbf{V} \setminus \mathbf{S}}$. Condition (2) holds because \mathbf{U} is exogenous; in $\mathcal{G}_{\mathbf{V} \setminus \mathbf{W}, \mathbf{R}}$ no open path between \mathbf{R} and \mathbf{U} conditioned on $\mathbf{V} \setminus \mathbf{W}$ could exist. Condition (3) holds because \mathbf{A} is defined precisely as the set of variables in \mathbf{R} that are not descendants of \mathbf{T} and thus that are not descendants of \mathbf{U} ; any path between \mathbf{A} and \mathbf{U} is therefore blocked by a child or descendant of \mathbf{U} that acts as a collider on the path.

The following derivation applies to $Q[\mathbf{S}]$ in \mathcal{G} .

$$\begin{aligned}
 Q[\mathbf{S}] &:= P(\mathbf{s} \mid do(\mathbf{v} \setminus \mathbf{s})) \\
 &= P(\mathbf{s} \mid do(\mathbf{r}, \mathbf{v} \setminus \mathbf{w})) \\
 &= \sum_{\mathbf{u}} P(\mathbf{s} \mid \mathbf{u}, \mathbf{r}, do(\mathbf{v} \setminus \mathbf{w})) P(\mathbf{u} \mid do(\mathbf{r}, \mathbf{v} \setminus \mathbf{w})) && \text{by (1)} \\
 &= \sum_{\mathbf{u}} P(\mathbf{s} \mid \mathbf{u}, \mathbf{r}, do(\mathbf{v} \setminus \mathbf{w})) P(\mathbf{u} \mid do(\mathbf{v} \setminus \mathbf{w})) && \text{by (2)} \\
 &= \sum_{\mathbf{u}} P(\mathbf{s} \mid \mathbf{u}, \mathbf{a}, \mathbf{b}, do(\mathbf{v} \setminus \mathbf{w})) P(\mathbf{u} \mid \mathbf{a}, do(\mathbf{v} \setminus \mathbf{w})) && \text{by (3)} \\
 &\geq \sum_{\mathbf{u}} P(\mathbf{s} \mid \mathbf{u}, \mathbf{a}, \mathbf{b}, do(\mathbf{v} \setminus \mathbf{w})) P(\mathbf{u}, \mathbf{b} \mid \mathbf{a}, do(\mathbf{v} \setminus \mathbf{w})) \\
 &= P(\mathbf{s}, \mathbf{b} \mid \mathbf{a}, do(\mathbf{v} \setminus \mathbf{w})) \\
 &= \frac{P(\mathbf{w} \mid do(\mathbf{v} \setminus \mathbf{w}))}{\sum_{\mathbf{s}, \mathbf{b}} P(\mathbf{w} \mid do(\mathbf{v} \setminus \mathbf{w}))} \\
 &= \frac{Q[\mathbf{W}]}{\sum_{\mathbf{s}, \mathbf{b}} Q[\mathbf{W}]}.
 \end{aligned}$$

The inequality follows from the fact that the event $\{\mathbf{u}, \mathbf{b}\}$ is less likely than event $\{\mathbf{u}\}$ under any probability. Finally, $Q[\mathbf{S}]$ is a function of $Pa(\mathbf{S})_{\mathcal{G}}$ only and thus this bound holds for any value of $\mathbf{Z} := Pa(\mathbf{W})_{\mathcal{G}} \setminus Pa(\mathbf{S})_{\mathcal{G}}$ and therefore any $\mathbf{Z} = \text{PossPa}(\mathbf{W})_{\mathcal{P}} \setminus \text{PossPa}(\mathbf{S})_{\mathcal{P}}$. In particular,

$$Q[\mathbf{S}] \geq \max_{\mathbf{z}} \frac{Q[\mathbf{W}]}{\sum_{\mathbf{s}, \mathbf{b}} Q[\mathbf{W}]}.$$

□

Prop. 3 restated. Given a PAG \mathcal{P} , consider sets $\mathbf{S} \subset \mathbf{C} \subseteq \mathbf{V}$ and let a partial topological ordering \mathbf{S} be $\mathbf{S}_1 < \dots < \mathbf{S}_k$. Define $\mathbf{W} = \text{PossAn}(\mathbf{S})_{\mathcal{P}_{\mathbf{C}}}$, $\mathbf{R} = \mathbf{W} \setminus \mathbf{S}$, $\mathbf{T} = \text{PossSp}(\mathbf{S})_{\mathcal{P}_{\mathbf{C}}} \setminus \mathbf{S}$, and $\mathbf{U} = \text{PossSp}(\mathbf{S})_{\mathcal{P}_{\mathbf{C}}} \setminus \mathbf{S}$. Let \mathbf{A}, \mathbf{B} partition \mathbf{R} such that $\mathbf{B} = \text{PossDe}(\mathbf{T})_{\mathcal{P}_{\mathbf{C}}} \cap \mathbf{R}$, $\mathbf{A} = \mathbf{R} \setminus \mathbf{B}$. $Q[\mathbf{S}]$ is upper bounded as follows:

$$Q[\mathbf{S}] \leq \min_{\mathbf{z}} \left\{ \frac{Q[\mathbf{W}]}{\sum_{\mathbf{s}, \mathbf{b}} Q[\mathbf{W}]} - \sum_{\mathbf{s}_k} \frac{Q[\mathbf{W}]}{\sum_{\mathbf{s}, \mathbf{b}} Q[\mathbf{W}]} \right\} + Q[\mathbf{S} \setminus \mathbf{S}_k], \quad (19)$$

where $\mathbf{Z} = \text{PossPa}(\mathbf{W})_{\mathcal{P}} \setminus \text{PossPa}(\mathbf{S})_{\mathcal{P}}$.

Proof. Similarly to the proof of Prop. 2 above, to show the claim we show that $Q[\mathbf{S}]$ is upper bounded in every causal diagram compatible with $\tilde{\mathcal{P}}$ and rely on facts (1,2,3) above. Let \mathcal{G} be any such causal diagram. Let a partial topological ordering of \mathbf{S} be $\mathbf{S}_1 < \dots < \mathbf{S}_k$.

It then holds that,

$$\begin{aligned}
 Q[\mathbf{S}] &:= P(\mathbf{s} \mid do(\mathbf{v} \setminus \mathbf{s})) \\
 &= P(\mathbf{s} \mid do(\mathbf{r}, \mathbf{v} \setminus \mathbf{w})) \\
 &= \sum_{\mathbf{u}} P(\mathbf{s} \mid \mathbf{u}, \mathbf{r}, do(\mathbf{v} \setminus \mathbf{w})) P(\mathbf{u} \mid do(\mathbf{r}, \mathbf{v} \setminus \mathbf{w})) \\
 &= \sum_{\mathbf{u}} P(\mathbf{s} \mid \mathbf{u}, \mathbf{r}, do(\mathbf{v} \setminus \mathbf{w})) P(\mathbf{u} \mid do(\mathbf{v} \setminus \mathbf{w})) \\
 &= \sum_{\mathbf{u}} P(\mathbf{s} \mid \mathbf{u}, \mathbf{a}, \mathbf{b}, do(\mathbf{v} \setminus \mathbf{w})) P(\mathbf{u} \mid \mathbf{a}, do(\mathbf{v} \setminus \mathbf{w})) \\
 &= \sum_{\mathbf{u}} P(\mathbf{s} \mid \mathbf{u}, \mathbf{a}, \mathbf{b}, do(\mathbf{v} \setminus \mathbf{w})) \left(P(\mathbf{u}, \mathbf{b} \mid \mathbf{a}, do(\mathbf{v} \setminus \mathbf{w})) + P(\mathbf{u} \mid \mathbf{a}, do(\mathbf{v} \setminus \mathbf{w})) - P(\mathbf{u}, \mathbf{b} \mid \mathbf{a}, do(\mathbf{v} \setminus \mathbf{w})) \right) \\
 &\stackrel{(1)}{=} \frac{Q[\mathbf{W}]}{\sum_{\mathbf{s}, \mathbf{b}} Q[\mathbf{W}]} + \sum_{\mathbf{u}} P(\mathbf{s} \mid \mathbf{u}, \mathbf{a}, \mathbf{b}, do(\mathbf{v} \setminus \mathbf{w})) \left(P(\mathbf{u} \mid \mathbf{a}, do(\mathbf{v} \setminus \mathbf{w})) - P(\mathbf{u}, \mathbf{b} \mid \mathbf{a}, do(\mathbf{v} \setminus \mathbf{w})) \right) \\
 &\stackrel{(2)}{\leq} \frac{Q[\mathbf{W}]}{\sum_{\mathbf{s}, \mathbf{b}} Q[\mathbf{W}]} + \sum_{\mathbf{u}} P(\mathbf{s} \setminus \mathbf{s}_k \mid \mathbf{u}, \mathbf{a}, \mathbf{b}, do(\mathbf{v} \setminus \mathbf{w})) \left(P(\mathbf{u} \mid \mathbf{a}, do(\mathbf{v} \setminus \mathbf{w})) - P(\mathbf{u}, \mathbf{b} \mid \mathbf{a}, do(\mathbf{v} \setminus \mathbf{w})) \right) \\
 &\stackrel{(3)}{=} \frac{Q[\mathbf{W}]}{\sum_{\mathbf{s}, \mathbf{b}} Q[\mathbf{W}]} + \sum_{\mathbf{u}} P(\mathbf{s} \setminus \mathbf{s}_k \mid \mathbf{u}, \mathbf{a}, \mathbf{b}, do(\mathbf{v} \setminus \mathbf{w}, \mathbf{s}_k)) P(\mathbf{u} \mid \mathbf{a}, do(\mathbf{v} \setminus \mathbf{w}, \mathbf{s}_k)) \\
 &\quad - \sum_{\mathbf{u}, \mathbf{s}_k} P(\mathbf{s} \mid \mathbf{u}, \mathbf{a}, \mathbf{b}, do(\mathbf{v} \setminus \mathbf{w})) P(\mathbf{u}, \mathbf{b} \mid \mathbf{a}, do(\mathbf{v} \setminus \mathbf{w})) \\
 &\stackrel{(4)}{=} \frac{Q[\mathbf{W}]}{\sum_{\mathbf{s}, \mathbf{b}} Q[\mathbf{W}]} + P(\mathbf{s} \setminus \mathbf{s}_k \mid \mathbf{a}, do(\mathbf{v} \setminus \mathbf{w}, \mathbf{b}, \mathbf{s}_k)) - \sum_{\mathbf{s}_k} \frac{Q[\mathbf{W}]}{\sum_{\mathbf{s}, \mathbf{b}} Q[\mathbf{W}]} \\
 &\stackrel{(5)}{=} \frac{Q[\mathbf{W}]}{\sum_{\mathbf{s}, \mathbf{b}} Q[\mathbf{W}]} + P(\mathbf{s} \setminus \mathbf{s}_k \mid do(\mathbf{v} \setminus \mathbf{w}, \mathbf{a}, \mathbf{b}, \mathbf{s}_k)) - \sum_{\mathbf{s}_k} \frac{Q[\mathbf{W}]}{\sum_{\mathbf{s}, \mathbf{b}} Q[\mathbf{W}]} \\
 &\stackrel{(6)}{=} \frac{Q[\mathbf{W}]}{\sum_{\mathbf{s}, \mathbf{b}} Q[\mathbf{W}]} + Q[\mathbf{S} \setminus \mathbf{S}_k] - \sum_{\mathbf{s}_k} \frac{Q[\mathbf{W}]}{\sum_{\mathbf{s}, \mathbf{b}} Q[\mathbf{W}]} .
 \end{aligned}$$

The first four equalities follows from the observations (1,2,3) in the derivation of the lower bound; (1) follows from the derivation in the lower bound; (2) follows from the fact that the event $\{\mathbf{s}\}$ is less likely than event $\{\mathbf{s} \setminus \mathbf{s}_k\}$ under any probability and that the difference in brackets is greater or equal to zero; (3) follows by rule 3 of the do-calculus since \mathbf{S}_k is d -separated from $\mathbf{S} \setminus \mathbf{S}_k$ given $\mathbf{U}, \mathbf{A}, \mathbf{B}, \mathbf{V} \setminus \mathbf{W}$ in $\mathcal{G}_{\overline{\mathbf{S}_k, \mathbf{V} \setminus \mathbf{W}}}$ and since \mathbf{S}_k is d -separated from \mathbf{U} given \mathbf{A} in $\mathcal{G}_{\overline{\mathbf{S}_k, \mathbf{V} \setminus \mathbf{W}}}$; (4) follows by marginalizing out \mathbf{U} and similarly to (1); (5) follows by the rule 2 of do-calculus since $\mathbf{S} \setminus \mathbf{S}_k$ is d -separated from \mathbf{A} in $\mathcal{G}_{\overline{\mathbf{V} \setminus \mathbf{W}, \mathbf{B}, \mathbf{S}_k, \mathbf{A}}}$; (6) follows by the definition of $Q[\cdot]$.

Similarly $P(\mathbf{s} \mid do(\mathbf{v} \setminus \mathbf{s}))$ is a function of $Pa(\mathbf{S})_{\mathcal{G}}$ only and thus this bound holds for any value of $\mathbf{Z} := Pa(\mathbf{W})_{\mathcal{G}} \setminus Pa(\mathbf{S})_{\mathcal{G}}$. In particular,

$$Q[\mathbf{S}] \leq \min_{\mathbf{z}} \left\{ \frac{Q[\mathbf{W}]}{\sum_{\mathbf{s}, \mathbf{b}} Q[\mathbf{W}]} - \sum_{\mathbf{s}_k} \frac{Q[\mathbf{W}]}{\sum_{\mathbf{s}, \mathbf{b}} Q[\mathbf{W}]} \right\} + Q[\mathbf{S} \setminus \mathbf{S}_k].$$

□

Prop. 4 restated. Let $\mathbf{W} \subseteq \mathbf{C} \subset \mathbf{V}$ such that $\mathbf{W} = \text{PossAn}(\mathbf{W})_{\mathcal{P}_{\mathbf{C}}}$. Then, $Q[\mathbf{W}] = \sum_{\mathbf{c} \setminus \mathbf{w}} Q[\mathbf{C}]$.

Proof. By (Jaber et al., 2018a, Prop. 1), if X is an ancestor of Y in a causal diagram $\mathcal{G}_{\mathbf{C}}$, then X is a possible ancestor of Y in the PAG $\mathcal{P}_{\mathbf{C}}$. By the converse, if X is not a possible ancestor of Y $\mathcal{P}_{\mathbf{C}}$, then X is not an ancestor of Y in $\mathcal{G}_{\mathbf{C}}$. Let $\mathbf{W} \subseteq \mathbf{C} \subset \mathbf{V}$ such that $\mathbf{W} = \text{PossAn}(\mathbf{W})_{\mathcal{P}_{\mathbf{C}}}$. By (Jaber et al., 2018a, Prop. 1) therefore, no variable in $\mathbf{R} = \mathbf{C} \setminus \mathbf{W}$ being a possible ancestor of \mathbf{W} in $\mathcal{P}_{\mathbf{C}}$ implies that no variable in $\mathbf{R} = \mathbf{C} \setminus \mathbf{W}$ is an ancestor of \mathbf{W} in any ME causal diagram $\mathcal{G}_{\mathbf{C}}$. For any causal diagram $\mathcal{G}_{\mathbf{C}}$, by (Tian and Pearl, 2003, Lemma 3) $Q[\mathbf{W}] = \sum_{\mathbf{r}} Q[\mathbf{C}]$. Moreover, if $Q[\mathbf{C}]$ could be uniquely computed from $P(\mathbf{V})$ and \mathcal{P} , the $Q[\mathbf{W}]$ could be uniquely computed from $P(\mathbf{V})$ and \mathcal{P} . □

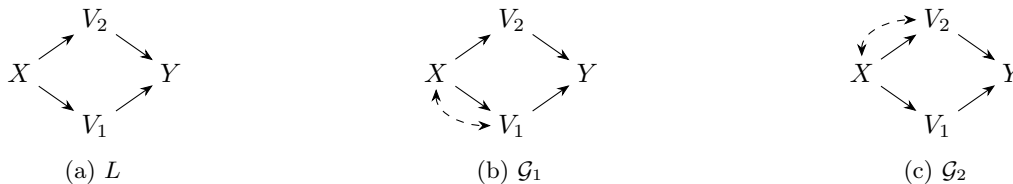


Figure 9: Second example of MBD causal diagrams used in the proof of Prop. 8.

respectively.). In contrast, in \mathcal{G}_2 : $P(y_1 | do(x)) = P(y_1 | x)$, $P(y_2 | do(x)) \in [P(y_2, x), P(y_2, x) + 1 - P(x)]$. The causal effect differs across \mathcal{G}_1 and \mathcal{G}_2 . Neither of the bounds computed from \mathcal{G}_1 or \mathcal{G}_2 include the other and therefore both have to be considered for correctly bounding causal effects from L .

Below we give two SCMs compatible with \mathcal{G}_1 whose causal effect $P(y_1 | do(x))$ evaluate to the lower and upper bounds obtained through posterior sampling illustrating the tightness of the returned bounds. Let $\mathcal{M}_1, \mathcal{M}_2 \in \mathbb{M}(\mathcal{G}_1)$ be defined by,

$$\mathcal{M}_1 := \begin{cases} x := f_X(u) \\ y_1 := \begin{cases} f_{Y_1}(x, u) & \text{if } x = f_X(u), \\ 1 & \text{otherwise.} \end{cases} \end{cases}$$

and,

$$\mathcal{M}_2 := \begin{cases} x := f_X(u) \\ y_1 := \begin{cases} f_{Y_1}(x, u) & \text{if } x = f_X(u), \\ 0 & \text{otherwise.} \end{cases} \end{cases}$$

For a $P_{\mathcal{M}_1}(u) = P_{\mathcal{M}_2}(u)$, both SCMs agree on observational distributions $P_{\mathcal{M}_1}(x, y_1) = P_{\mathcal{M}_2}(x, y_1)$. However the following derivations show that the interventional distribution $P(y_1 = 1 | do(x = 1))$ differs across models: for \mathcal{M}_1 equal to the analytical lower bound, and for \mathcal{M}_2 equal to the analytical upper bound demonstrating that (in this case) the bound is tight. In particular,

$$\begin{aligned} & P_{\mathcal{M}_1}(y_1 = 1 | do(x = 1)) \\ &= P_{\mathcal{M}_1}(y_1 = 1 | x = 1, u : x = f_X(u))P(u : x = f_X(u)) + P_{\mathcal{M}_1}(y_1 = 1 | x = 1, u : x = f_X(u))P(u : x = f_X(u)) \\ &= P(y_1 = 1 | x = 1)P(x = 1) \\ &= P(y_1 = 1, x = 1), \\ & P_{\mathcal{M}_2}(y_1 = 1 | do(x = 1)) \\ &= P_{\mathcal{M}_2}(y_1 = 1 | x = 1, u : x = f_X(u))P(u : x = f_X(u)) + P_{\mathcal{M}_2}(y_1 = 1 | x = 1, u : x = f_X(u))P(u : x = f_X(u)) \\ &= P(y_1 = 1 | x = 1)P(x = 1) + P_{\mathcal{M}_2}(y_1 = 1 | x = 1, u : x = f_X(u))P(u : x = f_X(u)) \\ &= P(y_1 = 1, x = 1) + 1 - P(x = 1). \end{aligned}$$

This holds also more generally for single output causal effect of the form $P(y | do(x))$. For instance, bounding $P(y | do(x))$ given the LEG L in Fig. 9a requires two MBD causal diagrams without loss of generality, given in Fig. 9b and Fig. 9c respectively. It could be shown by writing $P(y | do(x)) = \sum_{v_1, v_2} P(y | x, v_1, v_2)P(v_1, v_2 | do(x))$ that the upper bounds computed from \mathcal{G}_1 and \mathcal{G}_2 will disagree as upper bounds for $P(v_1, v_2 | do(x))$ will differ (as shown in the example above). \square

C Details on experiments

Sachs data is downloaded with the discretization procedure of (Hartemink et al., 2000), with 3 levels, from the bnlearn data repository.

The Lung Cancer data is generated from the following SCM compatible with the consensus causal diagram given in Fig. 4c. $P(u_C), P(u_L), P(u_A), P(u_D), P(u_P), P(u_T)$ are given by independent Gaussian distributions

Algorithm 2 Depth-first search

```

1: Input: LEG  $L$ 
2: Output: Set of Markov equivalent LEGs
3: Initialize  $S$  as an empty list and append  $L$ 
4: return Search( $L, S$ )

5: function Search( $L, S$ )
6:   for each  $L'$  obtained by performing a legitimate edge reversal do
7:     If  $L' \notin S$ , append  $L'$  to  $S$ 
8:     Run Search( $L', S$ )
9:   end for
10: return  $S$ 

```

with mean 0 and variance 1, and each observation (c, l, a, d, p, t) generated from exogenous variables using the structural assignments: $c \leftarrow \mathbb{1}\{u_C < 0\}$, $l \leftarrow \mathbb{1}\{c - u_L > 0\}$, $a \leftarrow \mathbb{1}\{u_A > 0\}$, $d \leftarrow \mathbb{1}\{l + a - 2u_d + 0.2p - 0.3T > -0.5\}$, $p \leftarrow \mathbb{1}\{u_P > 0\}$, $t \leftarrow \mathbb{1}\{u_T > 0\}$. The ground truth value of the causal effect is given by setting $c \leftarrow 1$ and evaluating $P(d = 1)$ under this updated model.

D Further discussion on enumeration strategies

One approach for enumerating Markov equivalent LEGs can be derived from the transformational characterization in Prop. 9 by reversal of directed edges. In particular, the following depth-first-search program (similarly to how one could enumerate all Markov equivalent DAGs with covered edge reversals (Wienöbst et al., 2023)) always terminates.

1. Let S be an empty list
2. Append L to S
3. Run **search**(L, S)

Starting from an LEG L , all neighbors of L (graphs with a single reversed edge) are explored and this is continued recursively. Eventually all ME LEGs are reached by Prop. 9 above. In order to not visit any LEG twice, it is necessary to store a set of all visited LEGs. An algorithm implementing this procedure is given in Alg. 2.

Proposition 10. *Alg. 2 enumerates a Markov equivalence class of LEGs and can be implemented with worst-case delay $\mathcal{O}(m^3)$, where m is the number of edges in any LEG of the equivalence class.*

Proof. The proof of (Wienöbst et al., 2023, Theorem 9) applies to the case of LEGs as the space of ME LEGs can be traversed by a sequence of edge traversals (starting from any LEG) as shown in (Zhang and Spirtes, 2012). □

Alg. 3 retrieves the set of MBD causal diagrams compatible with a given LEG. It proceeds by adding dashed bi-directed edges $X \dashleftrightarrow Y$ for every invisible edge between X and Y . When bi-directed edges for two adjacent invisible edges cannot be added without violating a conditional independence, two diagrams are constructed and the process continues along two separate branches of the tree. For example, $\{X \rightarrow Z \rightarrow Y\}$ creates $\{X \rightarrow Z \rightarrow Y, X \dashleftrightarrow Z\}$ and $\{X \rightarrow Z \rightarrow Y, Z \dashleftrightarrow Y\}$ separately as $\{X \rightarrow Z \rightarrow Y, X \dashleftrightarrow Z, Z \dashleftrightarrow Y\}$ violates the conditional independence between X and Y .

Proposition 11. *Alg. 3 enumerates all MBD causal diagrams compatible with a given LEG.*

Proof. In line (11), Alg. 3 appends and returns causal diagrams that can be constructed from a given LEG by adding the maximum number of bi-directed edges, *i.e.* diagrams without invisible edges and that therefore exclude any further unobserved confounding. Lines (9) and (12) ensure that all possible diagrams to which a bi-directed edge could be added are considered and ensures that all intermediate diagrams with invisible edges

Algorithm 3 Derivation of maximally bi-directed causal graphs

```

1: Input: LEG  $L$ 
2: Output: The set of maximally bi-directed graphs.
3: For all invisible edges of the form  $X \rightarrow Y$  such that  $X$  does not have any parents or spouses not adjacent to
    $Y$ , add a bi-directed edge  $X \leftrightarrow Y$  to  $L$ , creating a causal diagram  $\mathcal{G}$ 
4: Initialize an empty list  $S$  and append  $\mathcal{G}$  to it
5: Initialize an empty list  $S'$ 
6: while  $S$  is not empty do
7:   for each  $\mathcal{G}$  in  $S$  do
8:     Let  $k$  be the number of invisible edges in  $\mathcal{G}$ 
9:     Create graphs  $\mathcal{G}_1, \dots, \mathcal{G}_k$  by adding a bi-directed edge for each invisible edge in  $L$ 
10:    Mark visible edges in  $\mathcal{G}_1, \dots, \mathcal{G}_k$ 
11:    Append  $S'$  with the subset of  $\{\mathcal{G}_1, \dots, \mathcal{G}_k\}$  in which invisible edges do not exist
12:    Append  $S$  with the subset of  $\{\mathcal{G}_1, \dots, \mathcal{G}_k\}$  in which invisible edges do exist and remove  $\mathcal{G}$ 
13:   end for
14: end while
15: return  $S'$ 

```

are maintained for analysis. At termination therefore Alg. 3 will have enumerated all MBD causal diagrams compatible with a given LEG. □